

¹ Imposed form in the Early Acheulean? Evidence from Gona,
² Afar, Ethiopia

³ Dietrich Stout* Cheng Liu[†] Antoine Muller[‡] Michael J. Rogers[§]
⁴ Sileshi Semaw[¶]

⁵ 2023-09-23

⁶ **Abstract**

⁷ TBD.

⁸ **Keywords:** Gona; TBD; TBD; TBD; TBD; TBD; TBD

⁹ **Contents**

¹⁰ 1	Introduction	2
¹¹ 1.1	Identifying design	2
¹² 1.2	Measuring artifact form and modification	6
¹³ 1.3	The Early Acheulean at Gona	8
¹⁴ 2	Materials and Methods	9
¹⁵ 2.1	Materials	9
¹⁶ 2.2	Methods	9
¹⁷ 3	Results	11
¹⁸ 3.1	Measurement Validation	11
¹⁹ 3.2	Classification Validation	12
²⁰ 3.3	Effects of Reduction on Shape	13
²¹ References		14

*Department of Anthropology, Emory University, Atlanta, GA, USA; dwstout@emory.edu

[†]Department of Anthropology, Emory University, Atlanta, GA, USA; raylc1996@outlook.com

[‡]Institute of Archaeology, Mount Scopus, The Hebrew University of Jerusalem, Jerusalem, Israel; antoine.muller@mail.huji.ac.il

[§]Department of Anthropology, Southern Connecticut State University, New Haven, CT, USA; rogersm1@southernct.edu

[¶]Centro Nacional de Investigación sobre la Evolución Humana (CENIEH), Burgos, Spain; sileshi.semaw@cenieh.es

22 **1 Introduction**

23 The imposition of intended form on artifacts has long been viewed as a watershed in human
24 cognitive and cultural evolution and is most commonly associated with the emergence of “Large
25 Cutting Tools” (LCTs) in the Early Acheulean (Holloway, 1969; Isaac, 1976; Kuhn, 2021). However,
26 this interpretation of Acheulean LCTs as intentionally designed artifacts remains controversial.
27 Alternative proposals range from the possibility that LCTs were unintended by-products of flake
28 production (Moore & Perston, 2016; Noble & Davidson, 1996) to the suggestion that their form
29 was “at least partly under genetic control” (Corbey et al., 2016). Even accepting that LCT form
30 was to some extent intended, there is substantial disagreement over the specificity of design.
31 Some analyses have indicated that shape variation in Acheulean handaxes is largely a result of
32 resharpening (Iovita & McPherron, 2011; McPherron, 2000) whereas others find form to be unre-
33 lated to reduction intensity and more likely to reflect normative expectations of what handaxes
34 should look like (García-Medrano et al., 2019; Shipton & Clarkson, 2015b; Shipton & White, 2020).
35 Such debates about shape of Acheulean LCTs may appear narrowly technical but have broad
36 relevance for evolutionary questions including the origins of human culture (Corbey et al., 2016;
37 Shipton & Clarkson, 2015b; Tennie et al., 2017), language (Stout & Chaminade, 2012), teaching
38 (Gärdenfors & Höglberg, 2017), brain structure (Hecht et al., 2015), and cognition (Stout et al.,
39 2015; Wynn & Coolidge, 2016). To examine these questions, we studied the complete collection
40 of Early Acheulean flaked pieces from 5 sites at Gona Project Area and compared them with
41 Oldowan cores from 2 published sites at Gona. By comparing shape variation to measures of
42 flaking intensity and patterning, we sought to identify technological patterns that might reveal
43 intent.

44 **1.1 Identifying design**

45 There is a broad consensus that refined handaxes and cleavers from the later Acheulean resulted
46 from procedurally elaborate, skill intensive, and socially learned production strategies (Caruana,
47 2020; García-Medrano et al., 2019; Moore, 2020; Sharon, 2009; Shipton, 2019; Stout et al., 2014)
48 although debate over the presence of explicit, culturally transmitted shape preferences continues
49 (Iovita & McPherron, 2011; Moore, 2020; Shipton & White, 2020; Wynn & Gowlett, 2018). There is
50 much less agreement regarding the less heavily worked and formally standardized LCTs typical
51 of the earliest Acheulean (Beyene et al., 2013; Diez-Martín et al., 2015; Lepre et al., 2011; Semaw

52 et al., 2018; Torre & Mora, 2018). Such forms continue to occur with variable frequency in later
53 time periods (McNabb & Cole, 2015), and may be especially prevalent in eastern Asia (Li et al.,
54 2021). Although formal types have been recognized in the Early Acheulean and are commonly
55 used to describe assemblages, many workers now see a continuum of morphological variation
56 (Duke et al., 2021; Kuhn, 2021; Presnyakova et al., 2018) including the possibility that simple flake
57 production remained an important (Shea, 2010) or even primary (Moore & Perston, 2016) purpose
58 of Early Acheulean large core reduction.

59 Typologically, LCTs are differentiated from Mode 1 pebble cores on the basis of size (>10cm) and
60 shape (elongation and flattening) (e.g., Isaac, 1977). This consistent production of large, flat, and
61 elongated cores in the Achuelean has long been thought to reflect the pursuit of desired functional
62 and ergonomic properties for hand-held cutting tools (Wynn & Gowlett, 2018). Unplanned
63 flaking can sometimes produce cores that fall into the LCT shape range (Moore & Perston, 2016)
64 and this is one possible explanation of the relatively small “probifaces” that occur in low
65 frequencies in Oldowan assemblages (Isaac & Isaac, 1997). However, the Early Acheulean is
66 clearly distinguished from the Oldowan by the production of larger artifacts necessitating the
67 procurement and exploitation of larger raw material clasts. Although studies of handaxe variation
68 often focus on shape rather than size, this shift is an important aspect of artifact design with
69 relevance to both production and function.

70 Production of larger tools was accomplished either through a novel process of detaching and
71 working Large Flake Blanks (LFBs) from boulder cores or simply by using larger cobble and slab
72 cores (Isaac, 1969; Semaw et al., 2018; Torre & Mora, 2018). Both may involve similar flaking
73 “strategies” (e.g., bifacial or multifacial exploitation) to those present in the Oldowan (Duke et al.,
74 2021) but require more forceful percussion to detach larger flakes. This increases the perceptual
75 motor difficulty of the task (Stout, 2002) and in many cases may have been accomplished using
76 different percussive techniques and supports (Semaw et al., 2009). These new challenges would
77 have increased raw material procurement (Shea, 2010) and learning costs (Pargeter et al., 2019) as
78 well as the risk of serious injury (Gala et al., 2023) associated with tool production. This strongly
79 implies intentional pursuit of offsetting functional benefits related to size increase. These likely
80 included tool ergonomics and performance (Key & Lycett, 2017) as well as flake generation,
81 resharpening, and reuse potential (Shea, 2010). Early Acheulean LCT production is thus widely
82 seen as a part of shifting hominin behavioral ecological strategies including novel resources and

83 mobility patterns (Linares Matás & Yravedra, 2021; Rogers et al., 1994).

84 The degree of intentional design reflected in the shape of Early Acheulean LCTs is more difficult to
85 determine. For example, LFB production using a simple “least effort” bifacial/discoidal strategy
86 will tend to generate predominantly elongated (side or end struck) flakes (Toth, 1982) whether
87 or not this is an intentional design target. Similarly, the difficulty of flaking relatively spherical
88 cobbles (Toth, 1982) might bias initial clast selection and subsequent reduction toward flat and
89 elongated shapes even in the absence of explicit design targets. On the other hand, it has been
90 argued that the shape of Early Acheulean LFBs was intentionally predetermined using core
91 preparation techniques (Torre & Mora, 2018) and many researchers perceive efforts at intentional
92 shaping in the organization of flake scars on Early Acheulean handaxes and picks (Beyene et
93 al., 2013; Diez-Martín et al., 2015; Duke et al., 2021; Lepre et al., 2011; Semaw et al., 2009; Torre
94 & Mora, 2018). To date, however, the identification of Early Acheulean shaping has generally
95 relied on qualitative assessment by lithic analysts. Such assessment may in fact be reliable, but is
96 subject to concerns about potential selectivity, bias, and/or overinterpretation (Davidson, 2002;
97 Moore & Perston, 2016). Notably, a 3-dimensional morphometric (3DGM) study by Presnyakova,
98 et al. (2018) concluded that LCT shape variation in the Okote Member (~1.4 mya) at Koobi Fora
99 was largely driven by reduction intensity rather than different knapping strategies. However, this
100 study did not directly address the presence/absence of design targets constraining the observed
101 range of variation.

102 In later Acheulean contexts, reduction intensity effects are commonly equated with resharpening
103 and seen as an alternative to intentional form imposition (McPherron, 2000). Across heavily-
104 worked and relatively standardized LCT assemblages (e.g., Shipton & White, 2020), a *lack* of asso-
105 ciation between morphology and reduction intensity has been used as an argument-by-elimination
106 for the presence of imposed morphological norms or “mental templates” (García-Medrano et
107 al., 2019; Shipton et al., 2023; Shipton & Clarkson, 2015b). However, in the less heavily-worked
108 and more heterogeneous assemblages typical of the early Acheulean (Kuhn, 2021), it is equally
109 plausible that increasing reduction intensity would reflect degree of primary reduction rather
110 than subsequent resharpening (Archer & Braun, 2010). In this case, reduction intensity effects
111 on morphology would have the opposite interpretation: more reduction should result in closer
112 approximation of a desired form if such were present. For example, Beyene, et al. (2013) found
113 that increasing flake scar counts were associated with increasing handaxe refinement through

¹¹⁴ time at Konso, Ethiopia, which may reflect a more general trend in the African Acheulean ([Shipton, 2018](#)).
¹¹⁵

¹¹⁶ Interpretive approaches address this quandary by “reading” the organization of scars on individual
¹¹⁷ pieces to infer intent, but an adequate method to objectively quantify these insights has yet
¹¹⁸ to be developed. Current measures of reduction intensity, such as the scar density index (SDI)
¹¹⁹ ([Clarkson, 2013](#)), are designed to estimate total mass removed from a core and are reasonably
¹²⁰ effective ([Lombao et al., 2023](#)). However, mass removal was not the objective of Paleolithic flaking.
¹²¹ Indeed, knapping efficiency is usually conceived as generating an outcome while *minimizing*
¹²² required mass removal. This is true whether the desired outcome is a useful flake, a rejuvenated
¹²³ edge, or a particular core morphology. In simple flake production, mass removed is probably
¹²⁴ a good reflection of the completeness of exploitation (“exhaustion”) of cores and may have im-
¹²⁵ plications for required skill ([Pargeter et al., 2023; Toth, 1982](#)) as well as raw material economy
¹²⁶ ([Reeves et al., 2021; Shick, 1987](#)). However, in core shaping and resharpening, mass removal would
¹²⁷ typically represent an energetic and raw material cost to be minimized, and might even interfere
¹²⁸ with function ([Key, 2019](#)). Without further information, relationships between artifact shape and
¹²⁹ reduction intensity are thus open to conflicting interpretations as evidence of intentional design
¹³⁰ or its absence.

¹³¹ Li, et al. ([2015](#)) proposed a Flaked Area Index (FAI) as an alternative to SDI as a measure of
¹³² reduction intensity, arguing that its validity is supported by an observed correlation ($r=0.424$) with
¹³³ SDI. However, they also explain that “flaked area does not necessarily relate to the number of flake
¹³⁴ scars...a small number of large scars can produce a large area of scar coverage, and conversely, a
¹³⁵ large number of small scars can produce a small area of scar coverage.” (p. 6). We suggest that
¹³⁶ what FAI actually captures is the spatial extent modifications to the surface of a core. It is thus
¹³⁷ complementary to the measure of volume reduction provided by SDI and provides additional
¹³⁸ information to inform technological interpretations. For example, a correlation between FAI and
¹³⁹ artifact form without any effect of SDI would suggest a focus on “least-effort” shape imposition
¹⁴⁰ whereas the opposite pattern would be consistent with relatively intense resharpening of spatially
¹⁴¹ restricted areas on the core. A lack of shape correlation with either measure would be expected
¹⁴² for simple debitage with no morphological targets whereas a strong correlation with both would
¹⁴³ indicate a highly “designed” form achieved through extensive morphological and volumetric
¹⁴⁴ transformation. In the current study we thus considered SDI and FAI together in order to evaluate

¹⁴⁵ evidence of intentional shaping in the early Acheulean of Gona.

¹⁴⁶ 1.2 Measuring artifact form and modification

¹⁴⁷ Three-dimensional scanning and geometric morphometric (3DGM) methods are increasingly
¹⁴⁸ common in the study of LCT form and reduction intensity ([Archer & Braun, 2010](#); [Caruana, 2020](#);
¹⁴⁹ [Li et al., 2015, 2021](#); [Lycett et al., 2006](#); [Presnyakova et al., 2018](#); [Shipton & Clarkson, 2015b](#)).
¹⁵⁰ These methods provide high-resolution, coordinate-based descriptions of artifact form including
¹⁵¹ detailed information about whole object geometric relations that is not captured by conventional
¹⁵² linear measures ([Shott & Trail, 2010](#)). This includes measures of surface area used to compute
¹⁵³ both SDI and FAI measures ([Clarkson, 2013](#); [Li et al., 2015](#)). At the time of writing, however, 3D
¹⁵⁴ scans are available for only a small number of Gona artifacts, including 33 of the Oldowan and
¹⁵⁵ Acheulean flaked pieces used in this study ([Figure 1](#)). Despite continuing improvements, 3DGM
¹⁵⁶ methods still impose additional costs in terms of data collection and processing time as well as
¹⁵⁷ required equipment, software, and training. Importantly, 3DGM methods cannot be applied to
¹⁵⁸ pre-existing photographic and metric data sets (e.g., [Marshall et al., 2002](#)), including available
¹⁵⁹ data from Gona. For this reason, and to better understand the relative costs and benefits of
¹⁶⁰ 3DGM more generally, we sought to test the degree to which conventional measurements can
¹⁶¹ approximate 3DGM methods and produce reliable results by directly comparing our conventional
¹⁶² measures with 3DGM analysis of the 33 available scans.

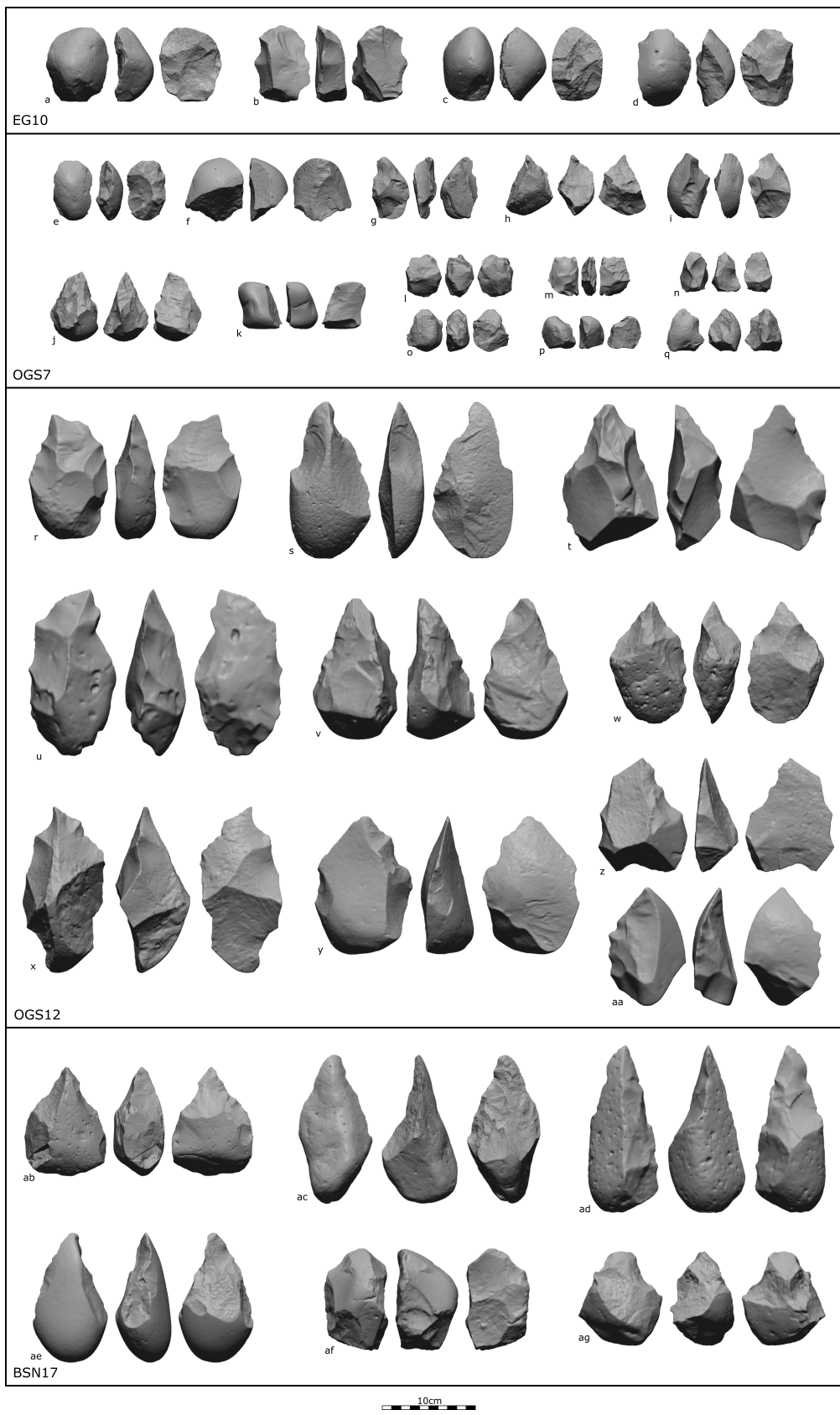


Figure 1: 3D Artifact scans from Gona used in this study.

163 For our study, we are specifically concerned with the accurate description of morphological
164 variation and estimation of artifact surface and flaked areas. With respect to morphology, we
165 were encouraged by the fact that aspects of form variation relevant to our research question (i.e.,
166 core elongation, flattening, and pointedness) are relatively simple to describe using sparse data.
167 3DGM studies of LCTs collect vast amounts of shape data but may discard upward of 50% of the
168 observed variation in order to focus on two or three interpretable principal components. Across
169 studies, these PCs consistently correspond to basic features like elongation, relative thickness,
170 pointedness, and position of maximum thickness that also emerge from lower-resolution spatial
171 data (Archer & Braun, 2010; García-Medrano et al., 2019; Lycett et al., 2006) and studies employing
172 linear measures rather than spatial coordinates (Crompton & Gowlett, 1993; Pargeter et al., 2019).
173 There is less evidence that conventional methods can accurately estimate artifact surface and
174 flaked areas. Clarkson (2013) advocated the use of 3D surface area measures as more accurate
175 than estimation from linear measures (e.g., surface area of a rectangular prism defined by artifact
176 dimensions). However, he also found that the error introduced by the linear approach was a
177 highly systematic, isometric overestimation of surface area and that results correlated with direct
178 3D measures with an impressive $r^2 = 0.944$ and no effect of variation in core shape. Insofar as
179 it is variation in the relationship between surface area and flaking intensity that is of interest,
180 rather than absolute artifact size, such systematic overestimation may not be problematic. Similar
181 concerns apply to the estimation of flaked area. Traditionally, such estimates have been done “by
182 eye” as a percentage of the total artifact surface (e.g., Dibble et al., 2005). Such estimations have
183 been found to be reasonably accurate when compared to 3D methods, but with the potential for
184 substantial error on individual artifacts (Lin et al., 2010). The accuracy of by-eye estimation has
185 yet to be systematically studied in Early Stone Age cores like those from Gona.

186 1.3 The Early Acheulean at Gona

187 Early Acheulean sites in the Gona Project area are distributed over a wide area within the Dana
188 Aoule North (DAN), Ounda Gona South (OGS), and Busidima North (BSN) drainages in the
189 Busidima Formation (Quade et al., 2004) and range in age from approximately 1.7 to 1.2 mya
190 (Semaw et al., 2018). The specific sites included in the current analysis are DAN-5, OGS-5, OGS-12,
191 and BSN-17, all estimated to ca. 1.7 – 1.4 mya by stratigraphic position in the Gona sequence
192 (Quade et al., 2008; Semaw et al., 2020). The Busidima Formation accumulated through fluvial
193 deposition by the ancestral Awash River (Type I context) and its smaller tributary channels (Type

194 II context) (Quade et al., 2004, 2008). Oldowan sites at Gona all occur in Type I sediments,
195 indicating channel bank/margin (OGS-7) or proximal floodplain (EG-10, EG-12) contexts close
196 to the large, hetero-lithic clasts available from point bars in the axial river channel (Quade et al.,
197 2004; Stout et al., 2005). Acheulean sites continue to occur in Type I contexts (BSN-17, DAN-5)
198 but are also found in Type II sediments (OGS-5, OGS-12,) reflecting increased utilization of large
199 perennial tributaries to the ancestral Awash River (Quade et al., 2008). Clasts locally available
200 in these tributaries were relatively small, implying that the large flakes and cobbles used to
201 produce Acheulean artifacts were initially sourced from the axial river. A similar pattern of habitat
202 diversification and increasing lithic transport distances has been described at other sites and
203 may be typical of the early Acheulean (Hay, 1976; Linares Matás & Yravedra, 2021; Rogers et
204 al., 1994). As with other early (i.e. >1.0 mya (Presnyakova et al., 2018; Stout, 2011)) Acheulean
205 assemblages, the Gona collections include numerous “crudely made” handaxes and picks on large
206 flake blanks and cobbles, as well as large (> 10cm) unmodified flakes, flaked pieces interpreted
207 typo-technologically as Mode 1 cores (see Figure 1af), and smallerdebitage (Semaw et al., 2018;
208 Semaw et al., 2020).

209 2 Materials and Methods

210 2.1 Materials

211 2.1.1 Archaeological Sample

212 Artifact collections analyzed here include *in situ* pieces excavated from intact stratigraphic
213 contexts and surface pieces systematically collected from the sediments eroding from these
214 layers. Surface pieces are included because the current technological analysis does not require
215 more precise spatial association, stratigraphic, and chronological control. Our sample comprises
216 the total collection of flaked pieces (Isaac & Isaac, 1997) and large (>10 cm) detached pieces from
217 each site, regardless of typo-technological interpretation.

218 2.2 Methods

219 2.2.1 Artifact Classification

220 Artifacts were classified according to initial form (pebble/cobble, detached piece, or indetermi-
221 nate), presence/absence of retouch, technological interpretation (“Mode 1” core vs. “Mode 2”

²²² LCT), and archaeological context (Oldowan vs. Early Acheulean sites). LCTs were additionally
²²³ classified as handaxes, knives, or picks following definitions from Kleindienst ([1962](#)). The validity
²²⁴ of technological interpretations and typological classifications was assessed through cluster
²²⁵ analysis based on artifact shape and reduction intensity variables.

²²⁶ **2.2.2 Artifact Measurement**

²²⁷ Conventional linear measures capture the direction (e.g., length > breadth) but not the location of
²²⁸ geometric relations (e.g., position of maximum breadth). We address this by collecting linear mea-
²²⁹ sures defined by homologous semi-landmarks. All artifacts were oriented along their maximum
²³⁰ dimension, which was measured and defined as “length.” The next largest dimension orthogonal
²³¹ to length was used to define the plane of “breadth,” with the dimension orthogonal to this plane
²³² defined as “thickness” Width (W_1, W_2, W_3) and thickness (T_1, T_2, T_3) measures were then collected
²³³ at 25%, 50%, and 75% of length, oriented so that 25% Width > 75% Width. To partition variation
²³⁴ in shape from variation in size, we divided all linear measures by the geometric mean ([Lycett et](#)
²³⁵ [al., 2006](#)). GM-transformed variables were then submitted to a Principal Components Analysis
²³⁶ (covariance matrix) to identify the main dimensions of shape variation.

²³⁷ Our semi-landmark measurement system allowed us to improve on the prism-based surface area
²³⁸ formula ($2LW + 2LT + 2WT$) by using our 7 recorded dimensions to more tightly fit three prisms
²³⁹ around the artifact: $SA = W_1T_1 + 2(.33L * W_1) + 2(.33L * T_1) + 2(.33L * W_2) + 2(.33L * T_2) + 2(.33L *$
²⁴⁰ $W_3) + 2(.33L * T_3) + W_3T_3$. Surface area calculated in this way correlates with mass^{2/3} at $r^2 = 0.947$
²⁴¹ in our sample. Calculated surface area was then used to derive the Scar Density Index: SDI =
²⁴² number of flake scars > 1cm per unit surface area ([Clarkson, 2013](#); [Shipton & Clarkson, 2015a](#)).
²⁴³ The Flaked Area Index (FAI: flaked area divided by total surface area) ([Li et al., 2015](#)) was estimated
²⁴⁴ directly “by eye” as a percentage of the total artifact surface.

²⁴⁵ **2.2.3 3D Methods**

²⁴⁶ Artifact scans (N=33) were cleaned, smoothed, and re-meshed using MeshLab. The 3D triangular
²⁴⁷ mesh of each scan was computed using Kazhdan and Hoppe’s ([2013](#)) method of screened Poisson
²⁴⁸ surface reconstruction in MeshLab. 3DGM analysis was conducted using the *AGMT3-D* program
²⁴⁹ of Herzlinger and Grosman ([2018](#)). Artifacts were automatically oriented according to the axis
²⁵⁰ of least asymmetry, then manually oriented in the interests of standardization with the length,

width, and thickness dimensions defined by the longest axis, followed by the next two longest axes perpendicular to the first. The wider end of the artifacts was positioned as the proximal end (base), and more protruding surfaces were oriented towards the user in the first orthogonal view. Then, a grid of 200 homologous semi-landmarks were overlain on each artifact's surface. Generalized Procrustes and Principal Component analyses were then undertaken to explore the shape variability of the sample. The surface area of each artifact was calculated using the *Artifact3-D* program of Grosman et al. (2022). *Artifact3-D* was also used to automatically identify the flake scar boundaries and compute each scar's surface area, using the scar analysis functions of Richardson et al. (2014).

2.2.4 Analyses

Measurement Validation: To assess the adequacy of shape descriptions based on our linear measures, we directly compared these with shape as quantified by 3D methods on the 33 artifacts for which scans are available. GM-transformed linear measures from these 33 artifacts were submitted to a variance-covariance matrix PCA. PCs with an eigenvalue greater than the mean were retained for analysis and the results compared qualitatively (morphological interpretation of PCs) and quantitatively (correlation of artifact factor scores) to 3D results. Accuracy of surface area and flaked area estimates was also assessed by correlation with 3D results.

3 Results

3.1 Measurement Validation

A PCA on GM transformed linear measures the 33 artifacts identified two PCs accounting for 75.6% of the variance. Linear-PC1 (Eigenvalue = 0.189) explained 55.2% of the variance. Factor loadings (**Table 1**) for Linear-PC1 reflect artifact elongation (i.e., an anti-correlation of length vs. distal width and thickness). This A PCA on GM transformed linear measures the 33 artifacts identified two PCs accounting for 75.6% of the variance. Linear-PC1 (Eigenvalue = 0.189) explained 55.2% of the variance. Factor loadings (**Table 1**) for Linear-PC1 reflect artifact elongation (i.e., an anti-correlation of length vs. distal width and thickness). This closely parallels the length vs. width and thickness tradeoff captured by 3DGM-PC1 (Figure 3a) and is reflected in a tight correlation of artifact scores produced by the two PCs ($r = 0.903$, $p < 0.001$, Figure 3c). Comparison with

Table 1: Component loadings for linear metric PCs .

Linear.metrics..GM.transformed.	Linear.PC1	Linear.PC2
Length	0.989	-0.107
W1	0.303	0.350
W2	0.403	0.767
W3	-0.176	0.790
T1	-0.135	-0.679
T2	-0.369	-0.623
T3	-0.607	-0.282

conventional shape ratios (Table 2) similarly indicates that both Linear-PC1 and 3DGM-PC1 largely capture variation in artifact elongation. A second factor (Linear-PC2, eigenvalue = 0.07) explained an additional 20.4% of variance. This factor was less strongly correlated with its 3DGM counterpart (3DGM-PC2; $r = 0.344$, $p = 0.050$) probably because Linear-PC2 describes anticorrelated variation in width and thickness (i.e., broad and flat vs. thick and pointed; Tables 1 & 2) whereas 3DGM-PC2 more purely isolates convergence (Table 2). The remainder of the shape variability explained by Linear-PC2 is captured by higher order 3DGM-PCs like 3DGM-PC3 to 5, which comprise the contribution of the left and right lateral margins to relative thickness. Including a third dimension in the GM analysis generates PCs that identify more specific shape attributes, but the underlying morphological variability captured by both the 2D and 3D analyses remains similar. Together, 3DGM-PC2 ($r = 0.344$, $p = 0.050$), 3DGM-PC3 ($r = -0.416$, $p = 0.016$), 3DGM-PC4 ($r = 0.458$, $p = 0.007$), and 3DGM-PC5 ($r = -0.352$, $p = 0.044$) correlate well with Linear-PC2, cumulatively capturing whether the items are broad and flat or thick and pointed.

3.2 Classification Validation

We first conducted a stepwise DFA on all flaked pieces ($n=192$) with inferred technological Mode (one vs. two) as the grouping variable and PCs 1 and 2, corrected SDI (cSDI), and FAI as the independent variables. All variables were retained, yielding one canonical DF (eigenvalue=1.825, Wilks Lambda = 0.354, $p < 0.001$) which correctly classified 93.8% of artifacts. We thus accepted the validity of classification by Mode in our sample and employed this distinction in subsequent analyses. There was no discernable difference in discriminant scores for Mode 1 cores from Oldowan ($n=37$) vs. Acheulean ($n=39$) contexts (, $p = 0.746$). Mode 1 cores from Oldowan contexts ($n=37$) do include 10 (27%) small, retouched flakes. Only one retouched flake from an Acheulean

301 context was classified by the DFA as a Mode 1 core. This piece, typologically classified as a “knife”,
302 is the smallest (93mm) retouched flake in the Acheulean sample. When retouched flakes are
303 excluded from the comparison, there are no significant differences in shape between Mode 1 cores
304 from Oldowan and Achuelean contexts. Interestingly, however, Acheulean Mode 1 cobble-cores
305 are much larger (mean weight 480g vs. 186g, Cohen’s d=1.137, p<0.001) and less heavily reduced
306 (mean cSDI 0.057 vs. 0.103, Cohen’s d = -0.884, p < 0.001) despite having similar FAI (mean 0.52
307 vs. 0.46, Cohen’s d=0.271, p=0.266).

308 Next, we conducted a stepwise DFA on all flaked Mode 2 pieces (i.e. excluding unmodified large
309 flakes, n = 115) with typology (handaxe, pick, knife) as the grouping variable and the same four
310 independent variables. Both shape PCs and FAI were retained, while cSDI was not entered.
311 This produced two DFs (DF1: Eigenvalue=1.536, 91.3% of variance; DF2: Eigenvalue = 0.146,
312 8.7% of variance; Wilks Lambda = 0.344; p<0.001) which correctly classified 71.3% of artifacts.
313 Inspection of DF coefficients shows that DF1 captures an inverse correlation between flaked area
314 and pointedness (Linear-PC2) whereas DF2 captures a positive relationship between flaked area
315 and elongation (Linear-PC2). A bivariate plot (Figure 5) illustrates the fact that DF1 captures
316 a range of variation from pointed, heavily-worked picks, through handaxes, to knives, with
317 substantial overlap between adjacent types (Table 2). As an intermediate type, “handaxes” were
318 correctly classified only 43.9% of the time. In agreement with others (Duke, et al., 2021, Kuhn,
319 2021, Presnyakova, et al., 2018) we conclude that these typological labels artificially partition a
320 continuum of variation and abandon them in subsequent analyses.

321 **3.3 Effects of Reduction on Shape**

322 To assess the influence of flake removals on core form, we examined the association between
323 our reduction measures (cSDI and FAI) and core shape (PC1, PC2). In the complete sample of
324 flaked pieces (n=192), we observed weak but significant effects of cSDI ($r=-0.294$, $p < 0.001$) and
325 FAI ($r=-0.294$, $p < 0.001$) on PC1(flatness) and of FAI only on PC2(pointedness) ($r=-0.436$, $p < 0.001$).
326 However, it is clear that these overall effects conflate different trends in Mode 1 vs. Mode 2 cores,
327 as well as in cores executed on flake vs. pebble/cobble bases. Within categories, we observed no
328 significant effects of cSDI whereas FAI had variable relationships with core form.

329 In Mode 1 cores, a weak negative effect of FAI on PC2(pointedness) ($n = 76$, $\beta = -0.006$, $r=0.240$,
330 $p = 0.037$) suggests that increasing extent of modification tends to slightly increase pointedness

³³¹ (Figure 6a). No effects of FAI on PC1 (flatness) or of SDIc on either PC approach significance. FAI
³³² and SDIc are moderately correlated ($\beta=0.001$, $r=0.524$, $p<0.001$), an effect that reflects increases
³³³ in the upper limit of scar density values as flaked area increases (i.e., flaked area constrains
³³⁴ maximum cSDI: Figure 6b).

³³⁵ In Mode 2 cores (n=115), reduction measures have different effects depending on initial blank
³³⁶ form. In general, the contrast between flat, lightly-worked flake bases and rounder, more-heavily
³³⁷ worked cobble bases tends to inflate relationships between FAI and core shape (Figure 7c,d).
³³⁸ Mode 2 cobble cores (n=37) display a negative effect of FAI on PC1(Flatness) ($\beta=-0.011$, $r=0.367$, p
³³⁹ = 0.026), no effect of FAI on pointedness, and no association between FAI and cSDI ($r=0.141$, p =
³⁴⁰ 0.406). Flake cores (n=69) show negative effects of FAI on PC1(Flatness) ($\beta=-0.007$, $r=0.284$, p =
³⁴¹ 0.018) and, more strongly, PC2(pointedness) ($\beta=-0.019$, $r=0.443$, $p < 0.001$). Flake cores show a
³⁴² small but significant positive effect of FAI on cSDI that, in contrast to Mode 1 cores, represents
³⁴³ actual covariance rather than simply a relaxation of constraint (i.e. both upper and lower limits
³⁴⁴ of cSDI increase with FAI). Comparison of Mode 2 flake cores with unmodified large flakes from
³⁴⁵ Achuelean contexts (n=35) shows that ranges of shape variation substantially overlap but that
³⁴⁶ flaking generally reduces both PC1(flatness) and PC2(pointedness). In fact, regressions of PC1
³⁴⁷ and PC2 on FAI show y-intercepts that closely approximate unmodified flake mean values (0.852
³⁴⁸ vs. 0.774 and 0.693 vs. 0.594, respectively) and significantly negative slopes as FAI increases (Figure
³⁴⁹ 9).

³⁵⁰ A small number of Mode 2 cores (n=9) were so heavily modified (mean FAI=89%, range 65-100)
³⁵¹ that the blank form could not be determined. These heavily worked “indeterminate” cores tend
³⁵² to show similar PC1(flatness) and PC2(pointedness) values to cobble-base cores (i.e. thicker and
³⁵³ more pointed than flake cores; Figure x). They also appear to follow general trends of shape
³⁵⁴ change with increasing FAI observed across base types (Figure 10).

³⁵⁵ References

- ³⁵⁶ Archer, W., & Braun, D. R. (2010). Variability in bifacial technology at Elandsfontein, Western cape,
³⁵⁷ South Africa: a geometric morphometric approach. *Journal of Archaeological Science*, 37(1),
³⁵⁸ 201–209. <https://doi.org/10.1016/j.jas.2009.09.033>
- ³⁵⁹ Beyene, Y., Katoh, S., WoldeGabriel, G., Hart, W. K., Uto, K., Sudo, M., Kondo, M., Hyodo, M.,
³⁶⁰ Renne, P. R., Suwa, G., & Asfaw, B. (2013). The characteristics and chronology of the earliest

- 361 Acheulean at Konso, Ethiopia. *Proceedings of the National Academy of Sciences*, 110(5), 1584–
362 1591. <https://doi.org/10.1073/pnas.1221285110>
- 363 Caruana, M. V. (2020). South African handaxes reloaded. *Journal of Archaeological Science: Reports*, 34, 102649. <https://doi.org/10.1016/j.jasrep.2020.102649>
- 365 Clarkson, C. (2013). Measuring core reduction using 3D flake scar density: a test case of changing
366 core reduction at Klasies River Mouth, South Africa. *Journal of Archaeological Science*, 40(12),
367 4348–4357. <https://doi.org/10.1016/j.jas.2013.06.007>
- 368 Corbey, R., Jagich, A., Vaesen, K., & Collard, M. (2016). The acheulean handaxe: More like a bird's
369 song than a beatles' tune? *Evolutionary Anthropology: Issues, News, and Reviews*, 25(1), 6–19.
370 <https://doi.org/10.1002/evan.21467>
- 371 Crompton, R. H., & Gowlett, J. A. J. (1993). Allometry and multidimensional form in Acheulean
372 bifaces from Kilombe, Kenya. *Journal of Human Evolution*, 25(3), 175–199. <https://doi.org/10.1006/jhev.1993.1043>
- 374 Davidson, I. (2002). *The Finished Artefact Fallacy: Acheulean Hand-axes and Language Origins* (A. Wray, Ed.; pp. 180–203). Oxford University Press. <https://rune.une.edu.au/web/handle/1959.11/1837>
- 377 Dibble, H. L., Schurmans, U. A., Iovita, R. P., & McLaughlin, M. V. (2005). The measurement and
378 interpretation of cortex in lithic assemblages. *American Antiquity*, 70(3), 545–560. <https://doi.org/10.2307/40035313>
- 380 Diez-Martín, F., Sánchez Yustos, P., Uribelarrea, D., Baquedano, E., Mark, D. F., Mabulla, A.,
381 Fraile, C., Duque, J., Díaz, I., Pérez-González, A., Yravedra, J., Egeland, C. P., Organista, E., &
382 Domínguez-Rodrigo, M. (2015). The Origin of The Acheulean: The 1.7 Million-Year-Old Site of
383 FLK West, Olduvai Gorge (Tanzania). *Scientific Reports*, 5(1), 17839. <https://doi.org/10.1038/srep17839>
- 385 Duke, H., Feibel, C., & Harmand, S. (2021). Before the Acheulean: The emergence of bifacial
386 shaping at Kokiselei 6 (1.8 Ma), West Turkana, Kenya. *Journal of Human Evolution*, 159, 103061.
387 <https://doi.org/10.1016/j.jhevol.2021.103061>
- 388 Gala, N., Lycett, S. J., Bebber, M. R., & Eren, M. I. (2023). The Injury Costs of Knapping. *American
389 Antiquity*, 1–19. <https://doi.org/10.1017/aaq.2023.27>
- 390 García-Medrano, P., Ollé, A., Ashton, N., & Roberts, M. B. (2019). The Mental Template in Handaxe
391 Manufacture: New Insights into Acheulean Lithic Technological Behavior at Boxgrove, Sussex,
392 UK. *Journal of Archaeological Method and Theory*, 26(1), 396–422. <https://doi.org/10.1007/s1>

- 393 **0816-018-9376-0**
- 394 Gärdenfors, P., & Höglberg, A. (2017). The archaeology of teaching and the evolution of homo
395 docens. *Current Anthropology*, 58(2), 188–208. <https://doi.org/10.1086/691178>
- 396 Grosman, L., Muller, A., Dag, I., Goldgeier, H., Harush, O., Herzlinger, G., Nebenhaus, K., Valetta,
397 F., Yashuv, T., & Dick, N. (2022). Artifact3-D: New software for accurate, objective and efficient
398 3D analysis and documentation of archaeological artifacts. *PLOS ONE*, 17(6), e0268401.
399 <https://doi.org/10.1371/journal.pone.0268401>
- 400 Hay, R. L. (1976). *Geology of the Olduvai Gorge: A study of sedimentation in a semiarid basin*.
401 University of California Press.
- 402 Hecht, E. E., Gutman, D. A., Khreisheh, N., Taylor, S. V., Kilner, J. M., Faisal, A. A., Bradley, B. A.,
403 Chaminade, T., & Stout, D. (2015). Acquisition of Paleolithic toolmaking abilities involves
404 structural remodeling to inferior frontoparietal regions. *Brain Structure & Function*, 220(4),
405 2315–2331. <https://doi.org/10.1007/s00429-014-0789-6>
- 406 Herzlinger, G., & Grosman, L. (2018). AGMT3-D: A software for 3-D landmarks-based geometric
407 morphometric shape analysis of archaeological artifacts. *PLOS ONE*, 13(11), e0207890. <https://doi.org/10.1371/journal.pone.0207890>
- 409 Holloway, R. L. (1969). Culture: A human domain. *Current Anthropology*, 10(4), 395–412. <https://www.jstor.org/stable/2740553>
- 411 Iovita, R., & McPherron, S. P. (2011). The handaxe reloaded: A morphometric reassessment
412 of Acheulian and Middle Paleolithic handaxes. *Journal of Human Evolution*, 61(1), 61–74.
413 <https://doi.org/10.1016/j.jhevol.2011.02.007>
- 414 Isaac, G. L. (1969). Studies of early culture in east africa. *World Archaeology*, 1(1), 1–28. <https://doi.org/10.1080/00438243.1969.9979423>
- 416 Isaac, G. L. (1976). Stages of Cultural Elaboration in the Pleistocene: Possible Archaeological
417 Indicators of the Development of Language Capabilities. *Annals of the New York Academy of
418 Sciences*, 280(1), 275–288. <https://doi.org/10.1111/j.1749-6632.1976.tb25494.x>
- 419 Isaac, G. L. (1977). *Olongesailie: Archaeological studies of a middle pleistocene lake basin in kenya*.
420 University of Chicago Press.
- 421 Isaac, G. L., & Isaac, B. (1997). *The stone artefact assemblages: A comparative study* (p. 262299).
- 422 Kazhdan, M., & Hoppe, H. (2013). Screened poisson surface reconstruction. *ACM Transactions on
423 Graphics*, 32(3), 29:129:13. <https://doi.org/10.1145/2487228.2487237>
- 424 Key, A. J. M. (2019). Handaxe shape variation in a relative context. *Comptes Rendus Palevol*, 18(5),

- 425 555–567. <https://doi.org/10.1016/j.crpv.2019.04.008>
- 426 Key, A. J. M., & Lycett, S. J. (2017). Influence of Handaxe Size and Shape on Cutting Efficiency: A
427 Large-Scale Experiment and Morphometric Analysis. *Journal of Archaeological Method and*
428 *Theory*, 24(2), 514–541. <https://doi.org/10.1007/s10816-016-9276-0>
- 429 Kleindienst, M. R. (1962). *Components of the east african acheulian assemblage: An analytic*
430 *approach*. 40, 81105.
- 431 Kuhn, S. L. (2021). *The evolution of paleolithic technologies*. Routledge.
- 432 Lepre, C. J., Roche, H., Kent, D. V., Harmand, S., Quinn, R. L., Brugal, J.-P., Texier, P.-J., Lenoble,
433 A., & Feibel, C. S. (2011). An earlier origin for the Acheulian. *Nature*, 477(7362), 82–85.
434 <https://doi.org/10.1038/nature10372>
- 435 Li, H., Kuman, K., & Li, C. (2015). Quantifying the Reduction Intensity of Handaxes with 3D
436 Technology: A Pilot Study on Handaxes in the Danjiangkou Reservoir Region, Central China.
437 *PLOS ONE*, 10(9), e0135613. <https://doi.org/10.1371/journal.pone.0135613>
- 438 Li, H., Lei, L., Li, D., Lotter, M. G., & Kuman, K. (2021). Characterizing the shape of Large Cutting
439 Tools from the Baise Basin (South China) using a 3D geometric morphometric approach.
440 *Journal of Archaeological Science: Reports*, 36, 102820. <https://doi.org/10.1016/j.jasrep.2021.102820>
- 441
- 442 Lin, S. C. H., Douglass, M. J., Holdaway, S. J., & Floyd, B. (2010). The application of 3D laser
443 scanning technology to the assessment of ordinal and mechanical cortex quantification in
444 lithic analysis. *Journal of Archaeological Science*, 37(4), 694–702. <https://doi.org/10.1016/j.jas.2009.10.030>
- 445
- 446 Linares Matás, G. J., & Yravedra, J. (2021). ‘We hunt to share’: Social dynamics and very large
447 mammal butchery during the oldowan–acheulean transition. *World Archaeology*, 53(2), 224–
448 254. <https://doi.org/10.1080/00438243.2022.2030793>
- 449 Lombao, D., Rabuñal, J. R., Cueva-Temprana, A., Mosquera, M., & Morales, J. I. (2023). Establishing
450 a new workflow in the study of core reduction intensity and distribution. *Journal of Lithic*
451 *Studies*, 10(2), 25 p.–25 p. <https://doi.org/10.2218/jls.7257>
- 452 Lycett, S. J., Cramon-Taubadel, N. von, & Foley, R. A. (2006). A crossbeam co-ordinate caliper
453 for the morphometric analysis of lithic nuclei: a description, test and empirical examples of
454 application. *Journal of Archaeological Science*, 33(6), 847–861. <https://doi.org/10.1016/j.jas.2005.10.014>
- 455
- 456 Marshall, G., Dupplaw, D., Roe, D., & Gamble, C. (2002). *Lower palaeolithic technology, raw*

- 457 material and population ecology (bifaces). Archaeology Data Service. <https://doi.org/10.5284/1000354>
- 458
- 459 McNabb, J., & Cole, J. (2015). The mirror cracked: Symmetry and refinement in the Acheulean
460 handaxe. *Journal of Archaeological Science: Reports*, 3, 100–111. <https://doi.org/10.1016/j.jasrep.2015.06.004>
- 461
- 462 McPherron, S. P. (2000). Handaxes as a Measure of the Mental Capabilities of Early Hominids.
463 *Journal of Archaeological Science*, 27(8), 655–663. <https://doi.org/10.1006/jasc.1999.0467>
- 464
- 465 Moore, M. W. (2020). Hominin Stone Flaking and the Emergence of ‘Top-down’ Design in Human
466 Evolution. *Cambridge Archaeological Journal*, 30(4), 647–664. <https://doi.org/10.1017/S0959774320000190>
- 467
- 468 Moore, M. W., & Perston, Y. (2016). Experimental Insights into the Cognitive Significance of Early
469 Stone Tools. *PLOS ONE*, 11(7), e0158803. <https://doi.org/10.1371/journal.pone.0158803>
- 470
- 471 Noble, W., & Davidson, I. (1996). *Human evolution, language and mind: A psychological and
472 archaeological inquiry*. Cambridge University Press.
- 473
- 474 Pargeter, J., Khreisheh, N., & Stout, D. (2019). Understanding stone tool-making skill acquisition:
475 Experimental methods and evolutionary implications. *Journal of Human Evolution*, 133,
476 146–166. <https://doi.org/10.1016/j.jhevol.2019.05.010>
- 477
- 478 Pargeter, J., Liu, C., Kilgore, M. B., Majoe, A., & Stout, D. (2023). Testing the Effect of Learning
479 Conditions and Individual Motor/Cognitive Differences on Knapping Skill Acquisition. *Journal
480 of Archaeological Method and Theory*, 30(1), 127–171. <https://doi.org/10.1007/s10816-022-09592-4>
- 481
- 482 Presnyakova, D., Braun, D. R., Conard, N. J., Feibel, C., Harris, J. W. K., Pop, C. M., Schlager, S.,
483 & Archer, W. (2018). Site fragmentation, hominin mobility and LCT variability reflected in
484 the early Acheulean record of the Okote Member, at Koobi Fora, Kenya. *Journal of Human
485 Evolution*, 125, 159–180. <https://doi.org/10.1016/j.jhevol.2018.07.008>
- 486
- 487 Quade, J., Levin, N. E., Simpson, S. W., Butler, R., McIntosh, W. C., Semaw, S., Kleinsasser, L.,
488 Dupont-Nivet, G., Renne, P., & Dunbar, N. (2008). *The geology of gona, afar, ethiopia* (J. Quade
489 & J. G. Wynn, Eds.; p. 131). Geological Society of America.
- 490
- 491 Quade, J., Levin, N., Semaw, S., Stout, D., Renne, P., Rogers, M., & Simpson, S. (2004). Paleoenvirons-
492 ments of the earliest stone toolmakers, gona, ethiopia. *GSA Bulletin*, 116(11-12), 1529–1544.
493 <https://doi.org/10.1130/B25358.1>
- 494
- 495 Reeves, J. S., Braun, D. R., Finestone, E. M., & Plummer, T. W. (2021). Ecological perspectives on

- 489 technological diversity at Kanjera South. *Journal of Human Evolution*, 158, 103029. <https://doi.org/10.1016/j.jhevol.2021.103029>
- 490
- 491 Richardson, E., Grosman, L., Smilansky, U., & Werman, M. (2014). *Extracting scar and ridge*
492 *features from 3D-scanned lithic artifacts* (A. Chrysanthi, C. Papadopoulos, D. Wheatley, G. Earl,
493 I. Romanowska, P. Murrieta-Flores, & T. Sly, Eds.; pp. 83–92). Amsterdam University Press.
494 <https://doi.org/10.1017/9789048519590.010>
- 495 Rogers, M. J., Harris, J. W. K., & Feibel, C. S. (1994). Changing patterns of land use by Plio-
496 Pleistocene hominids in the Lake Turkana Basin. *Journal of Human Evolution*, 27(1), 139–158.
497 <https://doi.org/10.1006/jhev.1994.1039>
- 498 Semaw, S., Rogers, M. J., Cáceres, I., Stout, D., & Leiss, A. C. (2018). *The Early Acheulean 1.6–1.2 Ma*
499 *from Gona, Ethiopia: Issues related to the Emergence of the Acheulean in Africa* (R. Gallotti & M.
500 Mussi, Eds.; pp. 115–128). Springer International Publishing. [https://doi.org/10.1007/978-3-319-75985-2_6](https://doi.org/10.1007/978-3-
501 319-75985-2_6)
- 502 Semaw, S., Rogers, M. J., Simpson, S. W., Levin, N. E., Quade, J., Dunbar, N., McIntosh, W. C.,
503 Cáceres, I., Stinchcomb, G. E., Holloway, R. L., Brown, F. H., Butler, R. F., Stout, D., & Everett, M.
504 (2020). Co-occurrence of acheulian and oldowan artifacts with homo erectus cranial fossils
505 from gona, afar, ethiopia. *Science Advances*, 6(10), eaaw4694. <https://doi.org/10.1126/sciadv.aaw4694>
- 506
- 507 Semaw, S., Rogers, M., & Stout, D. (2009). *The Oldowan-Acheulian Transition: Is there a “Developed*
508 *Oldowan” Artifact Tradition?* (M. Camps & P. Chauhan, Eds.; pp. 173–193). Springer. https://doi.org/10.1007/978-0-387-76487-0_10
- 509
- 510 Sharon, G. (2009). Acheulian giant-core technology: A worldwide perspective. *Current Anthropol-*
511 *ogy*, 50(3), 335–367. <https://doi.org/10.1086/598849>
- 512 Shea, J. J. (2010). *Stone Age Visiting Cards Revisited: A Strategic Perspective on the Lithic Technology*
513 *of Early Hominin Dispersal* (J. G. Fleagle, J. J. Shea, F. E. Grine, A. L. Baden, & R. E. Leakey, Eds.;
514 pp. 47–64). Springer Netherlands. https://doi.org/10.1007/978-90-481-9036-2_4
- 515 Shick, K. D. (1987). Modeling the formation of Early Stone Age artifact concentrations. *Journal of*
516 *Human Evolution*, 16(7), 789–807. [https://doi.org/10.1016/0047-2484\(87\)90024-8](https://doi.org/10.1016/0047-2484(87)90024-8)
- 517 Shipton, C. (2018). Biface Knapping Skill in the East African Acheulean: Progressive Trends and
518 Random Walks. *African Archaeological Review*, 35(1), 107–131. [https://doi.org/10.1007/s104 37-018-9287-1](https://doi.org/10.1007/s104
519 37-018-9287-1)
- 520 Shipton, C. (2019). The Evolution of Social Transmission in the Acheulean. In K. A. Overmann & F.

- 521 L. Coolidge (Eds.), *Squeezing Minds From Stones: Cognitive Archaeology and the Evolution of*
522 *the Human Mind* (pp. 332–354). Oxford University Press.
- 523 Shipton, C., & Clarkson, C. (2015a). Flake scar density and handaxe reduction intensity. *Journal of*
524 *Archaeological Science: Reports*, 2, 169–175. <https://doi.org/10.1016/j.jasrep.2015.01.013>
- 525 Shipton, C., & Clarkson, C. (2015b). Handaxe reduction and its influence on shape: An experimen-
526 tal test and archaeological case study. *Journal of Archaeological Science: Reports*, 3, 408–419.
527 <https://doi.org/10.1016/j.jasrep.2015.06.029>
- 528 Shipton, C., Groucutt, H. S., Scerri, E., & Petraglia, M. D. (2023). Uniformity and diversity in
529 handaxe shape at the end of the acheulean in southwest asia. *Lithic Technology*, 0(0), 1–14.
530 <https://doi.org/10.1080/01977261.2023.2225982>
- 531 Shipton, C., & White, M. (2020). Handaxe types, colonization waves, and social norms in the
532 British Acheulean. *Journal of Archaeological Science: Reports*, 31, 102352. <https://doi.org/10.1016/j.jasrep.2020.102352>
- 533 Shott, M. J., & Trail, B. W. (2010). Exploring new approaches to lithic analysis: Laser scanning and
534 geometric morphometrics. *Lithic Technology*, 35(2), 195–220. <https://doi.org/10.1080/01977261.2010.11721090>
- 535 Stout, D. (2002). Skill and cognition in stone tool production: An ethnographic case study from
536 irian jaya. *Current Anthropology*, 43(5), 693–722. <https://doi.org/10.1086/342638>
- 537 Stout, D. (2011). Stone toolmaking and the evolution of human culture and cognition. *Philoso-
538 sophical Transactions of the Royal Society B: Biological Sciences*, 366(1567), 1050–1059. <https://doi.org/10.1098/rstb.2010.0369>
- 539 Stout, D., Apel, J., Commander, J., & Roberts, M. (2014). Late Acheulean technology and cognition
540 at Boxgrove, UK. *Journal of Archaeological Science*, 41, 576–590. <https://doi.org/10.1016/j.jas.2013.10.001>
- 541 Stout, D., & Chaminade, T. (2012). Stone tools, language and the brain in human evolution.
542 *Philosophical Transactions of the Royal Society B: Biological Sciences*, 367(1585), 75–87. <https://doi.org/10.1098/rstb.2011.0099>
- 543 Stout, D., Hecht, E., Khriesheh, N., Bradley, B., & Chaminade, T. (2015). Cognitive Demands of
544 Lower Paleolithic Toolmaking. *PLOS ONE*, 10(4), e0121804. <https://doi.org/10.1371/journal.pone.0121804>
- 545 Stout, D., Quade, J., Semaw, S., Rogers, M. J., & Levin, N. E. (2005). Raw material selectivity of the
546 earliest stone toolmakers at Gona, Afar, Ethiopia. *Journal of Human Evolution*, 48(4), 365–380.

- 553 <https://doi.org/10.1016/j.jhevol.2004.10.006>
- 554 Tennie, C., Premo, L. S., Braun, D. R., & McPherron, S. P. (2017). Early stone tools and cultural
555 transmission: Resetting the null hypothesis. *Current Anthropology*, 58(5), 652–672. <https://doi.org/10.1086/693846>
- 556
- 557 Torre, I. de la, & Mora, R. (2018). Technological behaviour in the early Acheulean of EF-HR
558 (Olduvai Gorge, Tanzania). *Journal of Human Evolution*, 120, 329–377. <https://doi.org/10.101>
559 [j.jhevol.2018.01.003](https://doi.org/10.1016/j.jhevol.2018.01.003)
- 560 Toth, N. (1982). *The stone technologies of early hominids at koobi fora, kenya: An experimental*
561 *approach* [PhD thesis]. <https://www.proquest.com/docview/303067974/abstract/305CC66DA94A43EEPQ/1>
- 562
- 563 Wynn, T., & Coolidge, F. L. (2016). Archeological insights into hominin cognitive evolution.
564 *Evolutionary Anthropology: Issues, News, and Reviews*, 25(4), 200–213. <https://doi.org/10.100>
565 [2/evan.21496](https://doi.org/10.1002/evan.21496)
- 566 Wynn, T., & Gowlett, J. (2018). The handaxe reconsidered. *Evolutionary Anthropology: Issues,*
567 *News, and Reviews*, 27(1), 21–29. <https://doi.org/10.1002/evan.21552>